

Supplementary Materials

Facile synthesis of Ag/AgCl/PAF-54 heterojunction photocatalysts for TC degradation

Yonghui Lin, Letian Gan, Xiaojun Zhao^{*}, Guang Che, Shicheng Wang, Qinhe Pan^{*}

Key Laboratory of Advanced Materials of Tropical Island Resources, Ministry of Education, School of Chemistry and Chemical Engineering, Hainan University, Haikou 570228, China.

***Correspondence to:** Dr. Xiaojun Zhao, Prof. Qinhe Pan, Key Laboratory of Advanced Materials of Tropical Island Resources, Ministry of Education, School of Chemistry and Chemical Engineering, Hainan University, 58 Renmin Avenue, Haikou 570228, Hainan, China. E-mail: xiaojunzhao2013@163.com; panqinhe@163.com

MAIN TEXT (optional)

1. Materials

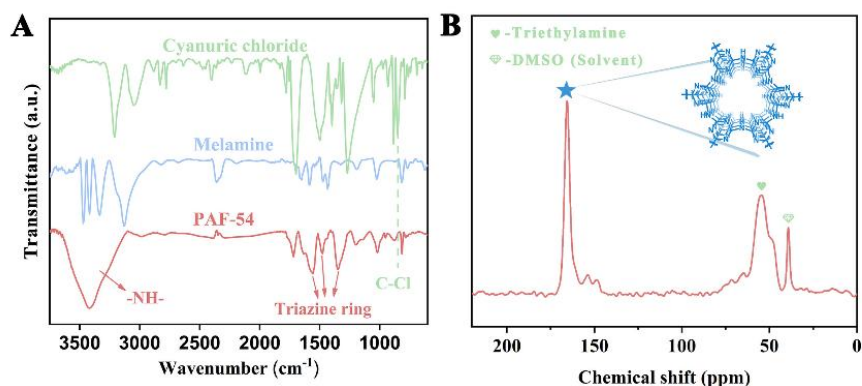
Cyanuric chloride, melamine, triethylamine (EtN₃), silver nitrate (AgNO₃), tetracycline (TC, 99%) and sodium borohydride (NaBH₄) were purchased from Aladdin Chemical Reagent Co., Ltd.

2. Characterization

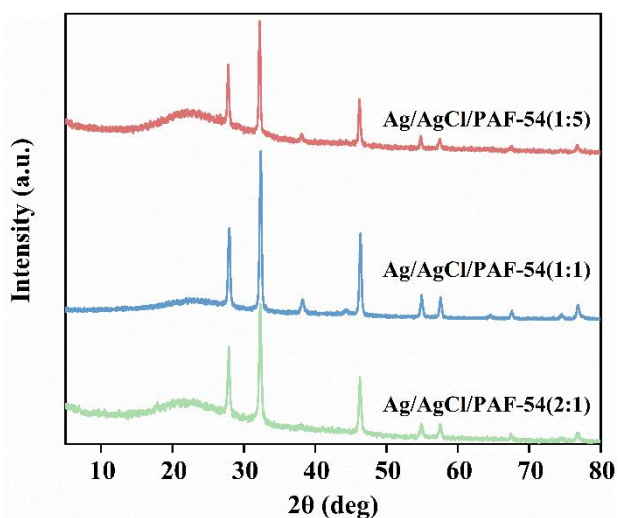
Powder X-ray diffraction (PXRD) was carried out at room temperature on a Rigaku Miniflex 600 X-ray diffractometer. Solid state ¹³C CP/MAS NMR was carried out using a Bruker Avance III HD in 400MHz. Fourier transform infrared (FT-IR) spectrum was tested on the Shimadzu IRAFINITY-1S infrared spectrometer with a range of 4000-500 cm⁻¹. Thermogravimetric analysis (TGA) was performed on the Rigaku Thermal plus EVO2 TG-DTA 8122 instrument under air atmosphere at a heating rate of 10 °C • min⁻¹. N₂-adsorption isotherms were obtained at 77 K using an JW-BK112. Micromorphology and element distribution were observed by Transmission electron microscope (TEM, thermoscientific Talos F200X G2). XPS was recorded on a Thermo ESCALAB 250Xi with Al K α (1486.6 eV). The elemental analyses were measured by an Agilent ICP-OES 730. Electron spin resonance spectroscopy (ESR, Bruker EMXPLUS) was used to identify the active radicals involved in the catalytic process. Ultraviolet-visible diffuse reflectance spectrum (UV-Vis DRS) was obtained using Lambda 750S in the range of 800-200 nm. The concentration of TC solution was tested with a UV-2700 UV-Vis spectrophotometer at 357 nm.

3. Electrochemical measurements

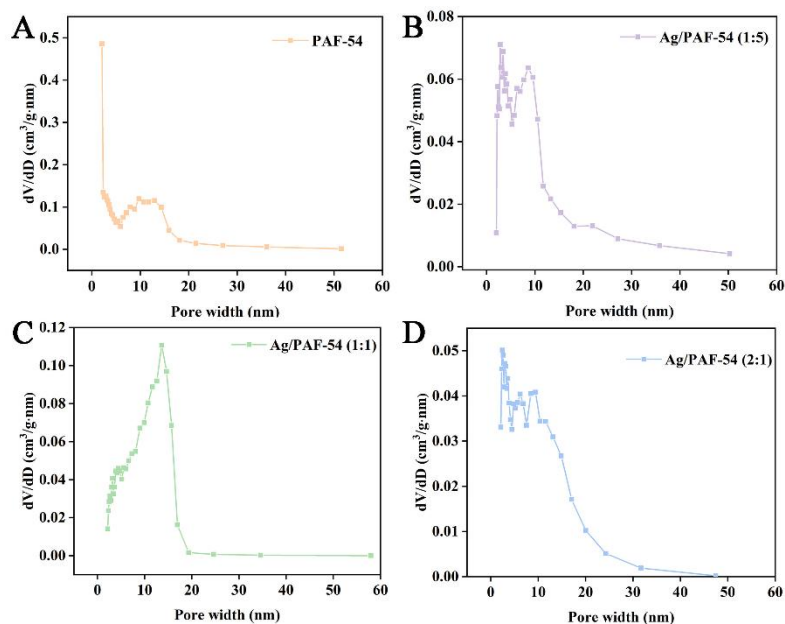
The photocurrent response, electrochemical impedance spectroscopy (EIS) and Mott-Schottky (M-S) curves were recorded using a standard three-electrode system on CHI660C electrochemical workstation in Shanghai, China. The catalyst sample is coated on indium tin oxide (ITO) glass as the working electrode. The working electrode was irradiated by 400nm cut-off filter under 300W xenon lamp with 0.5 M Na₂SO₄ aqueous solution as electrolyte. Pt foil and Ag/AgCl electrodes were used as counting and reference electrodes, respectively. To prepare the working electrode, the slurry consisted of 3 mg sample, 680 μ L water, 300 μ L ethanol, and 20 μ L Nafion. The slurry is then applied to the ITO glass with an exposure area of 1 cm² and dried at 65°C for 20 min.



Supplementary Figure 1. (A) FTIR spectra and (B) ^{13}C CPMAS NMR spectra of PAF-54. In the infrared spectrum of PAF-54, peaks near 1561 cm^{-1} , 1473 cm^{-1} , and 1342 cm^{-1} indicate the presence of a triazine ring. The presence of a wide characteristic peak (3390 cm^{-1}) belonging to the secondary amine and the obvious weakening of the C-Cl peak (841 cm^{-1}) indicate the polycondensation reaction between melamine and melamine chloride. In addition, the strong signal at 166 ppm in the ^{13}C CP-MASNMR spectrum came from the carbon of the triazine ring, further confirming the successful preparation of PAF-54.



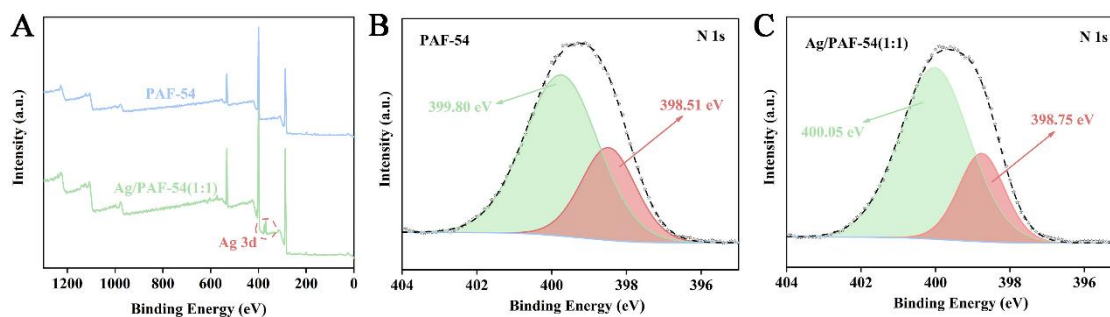
Supplementary Figure 2. PXRD pattern of Ag/AgCl/PAF-54(1:5), Ag/AgCl/PAF-54(1:1) and Ag/AgCl/PAF-54(2:1).



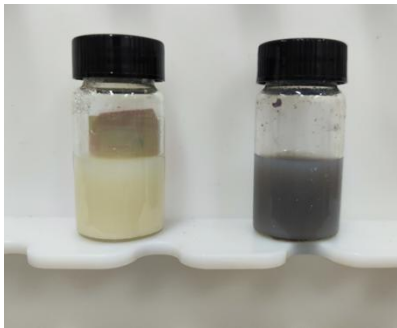
Supplementary Figure 3. Pore size distribution of (A) PAF-54, (B) Ag/AgCl/PAF-54(1:5), (C) Ag/AgCl/PAF-54(1:1) and (D) Ag/AgCl/PAF-54(2:1).

Supplementary Table 1. Physicochemical properties of different samples

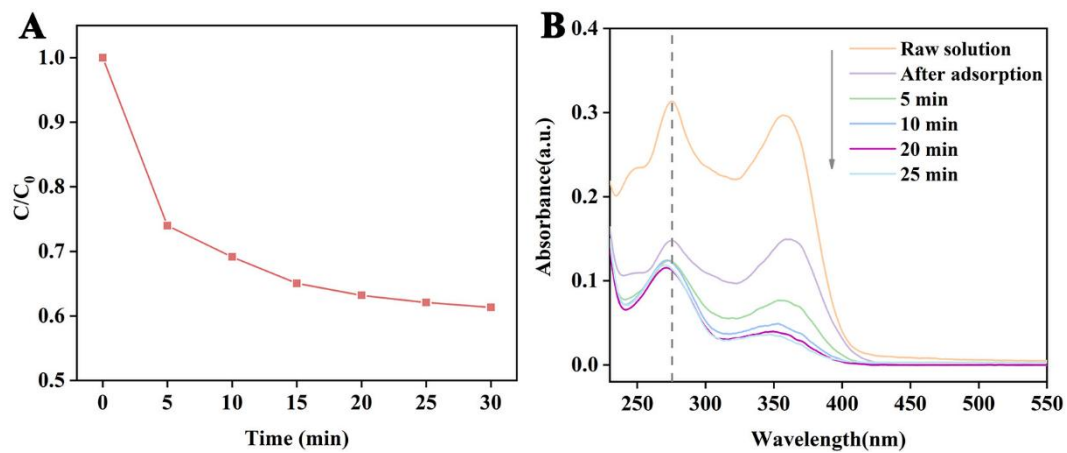
Sample	$S_{BET}(m^2/g)$	$V_{total}(cm^3/g)$	Average pore size
PAF-54	755.9	2.055	8.68
Ag/AgCl/PAF-54(1:5)	245.9	1.470	12.2
Ag/AgCl/PAF-54(1:1)	230.0	1.076	9.56
Ag/AgCl/PAF-54(2:1)	187.7	0.796	8.91



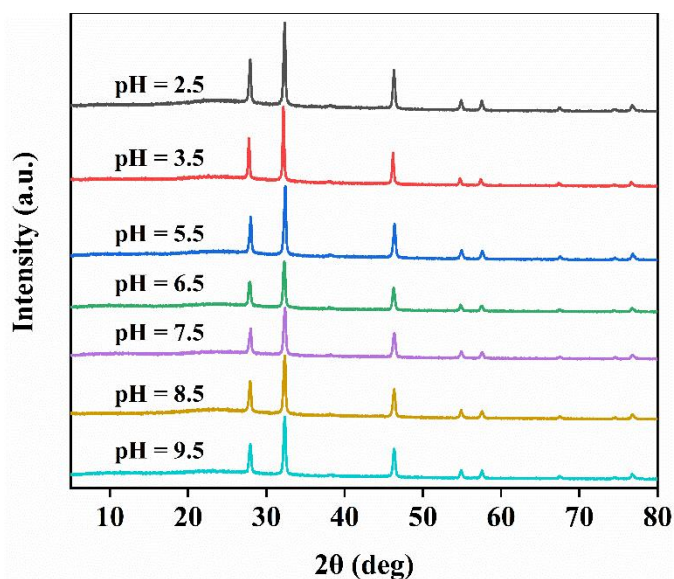
Supplementary Figure 4. XPS survey spectrum of (A) PAF-54 and Ag/AgCl/PAF-54(1:1). N 1s of (B) PAF-54 and (C) Ag/AgCl/PAF-54(1:1).



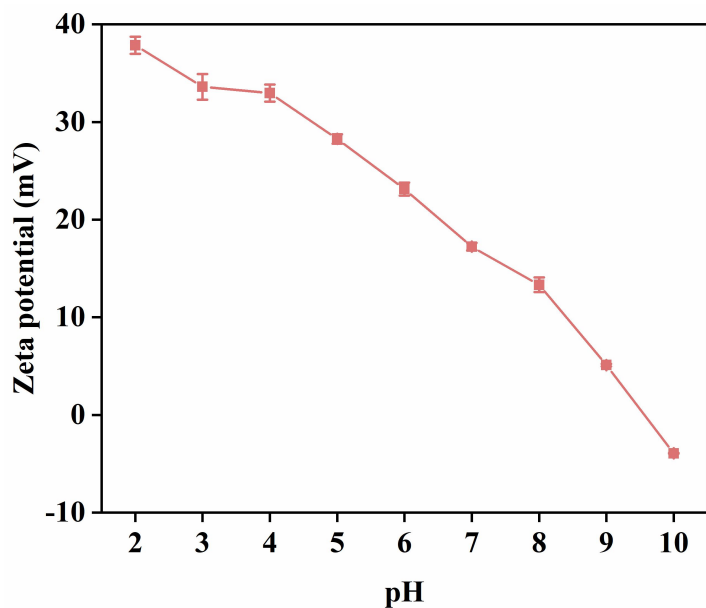
Supplementary Figure 5. Optical photos of Ag/AgCl/PAF-54(1:1) (right) and Ag/AgCl/PAF-54(Dark) (left).



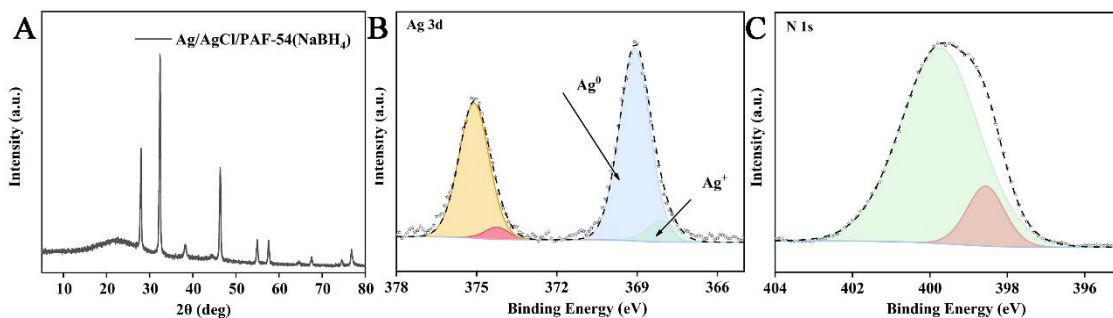
Supplementary Figure 6. (A) Adsorption of TC under dark by Ag/AgCl/PAF-54(1:1); (B) Ultraviolet absorption spectrum of solution after adsorption and degradation of TC.



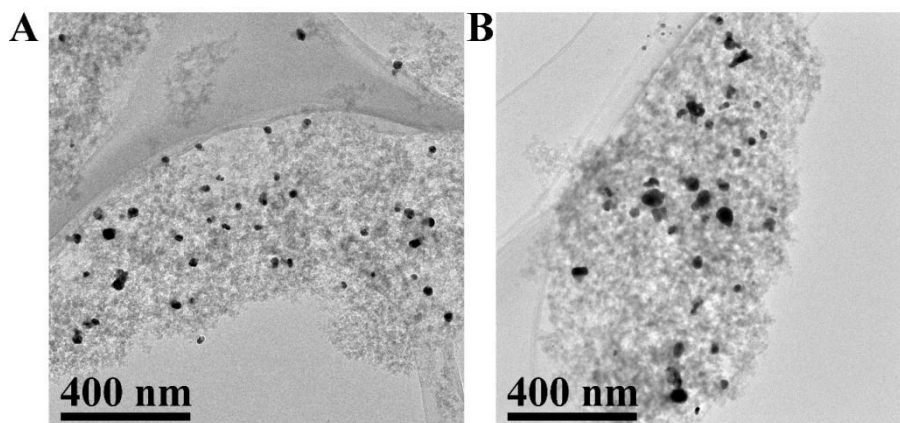
Supplementary Figure 7. PXRD pattern of Ag/AgCl/PAF-54 at different pH.



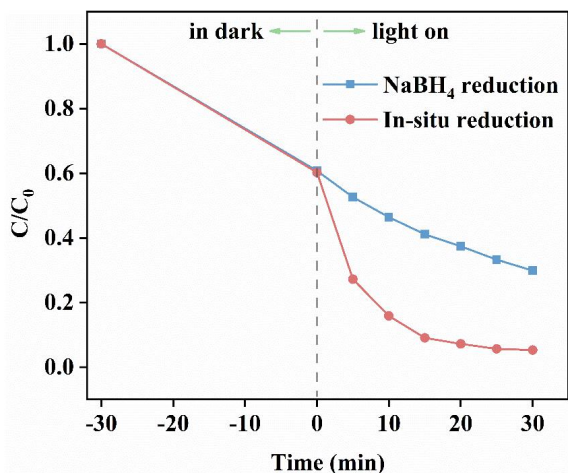
Supplementary Figure 8. Zeta Potential plots of Ag/AgCl/PAF-54(1:1).



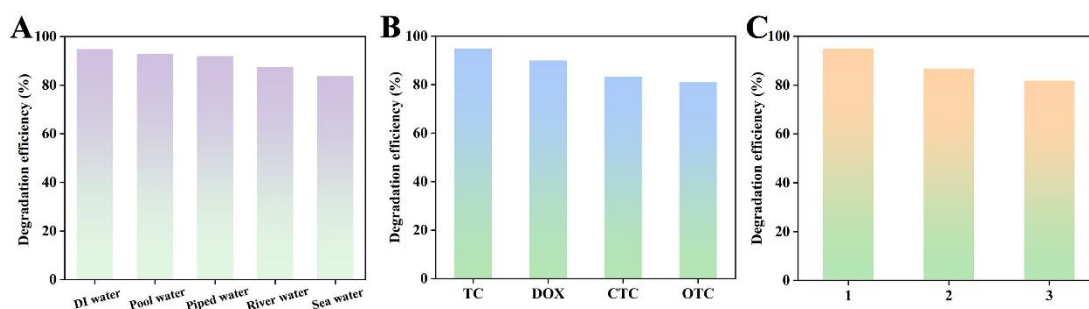
Supplementary Figure 9. (A) PXR D pattern; (B) Ag 3d; and (C) N 1s of Ag/AgCl/PAF-54(NaBH₄).



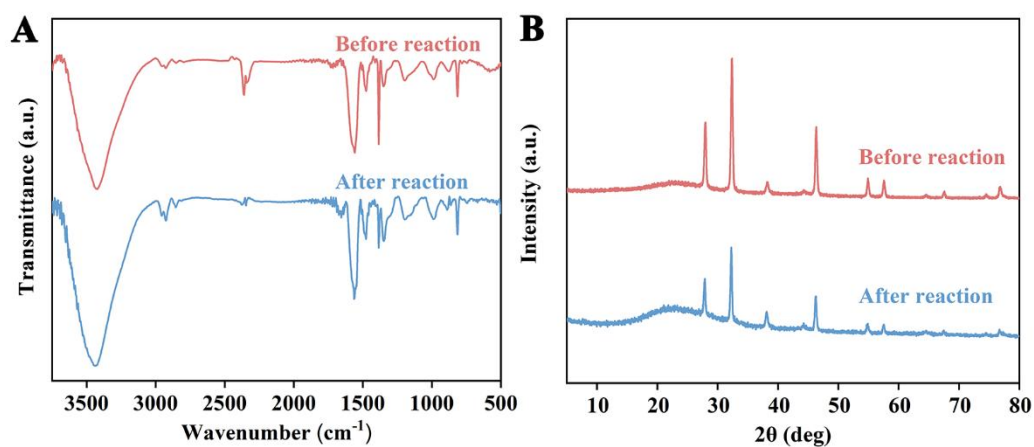
Supplementary Figure 10. TEM images of (A) Ag/AgCl/PAF-54(1:1); and (B) Ag/AgCl/PAF-54(NaBH₄).



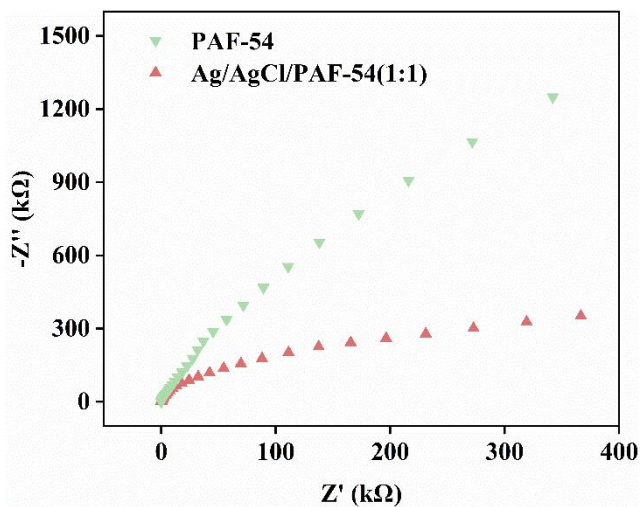
Supplementary Figure 11. Photocatalytic degradation efficiency of TC by Ag/AgCl/PAF-54 with different reduction methods.



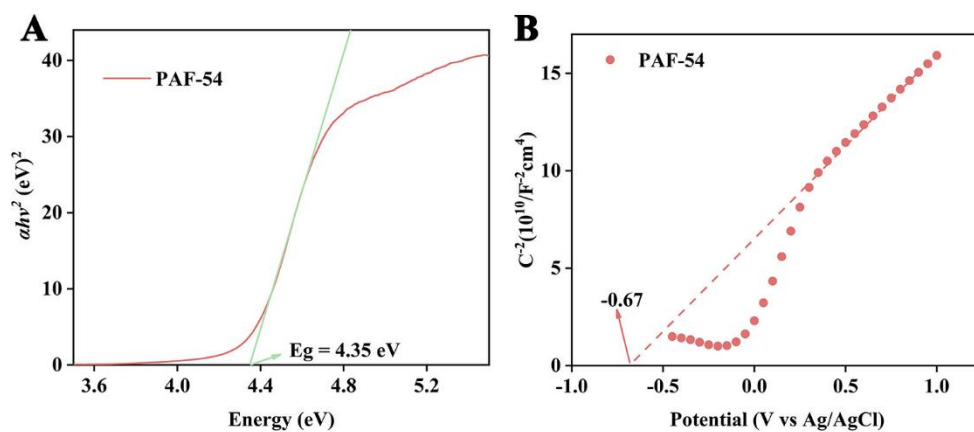
Supplementary Figure 12. (A) Photocatalytic degradation efficiency of TC in different water samples (spiked concentration of 10 mg/L); (B) Photocatalytic degradation of different kinds of tetracycline antibiotics; (C) Recycling tests of the TC photodegradation under visible light.



Supplementary Figure 13. (A) FTIR spectra and (B) PXRD pattern of Ag/AgCl/PAF-54(1:1) before and after reaction.

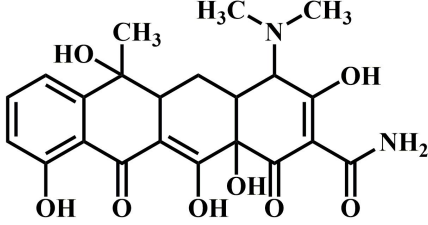
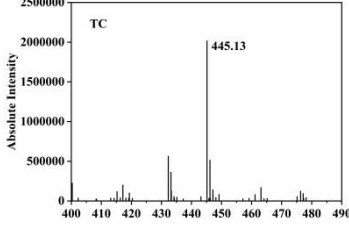
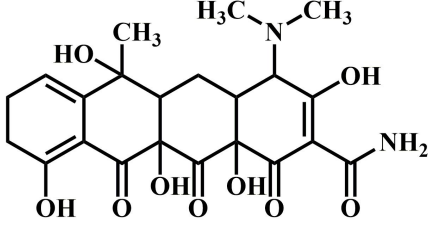
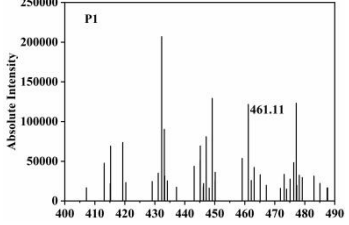
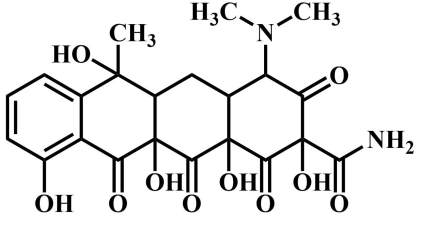
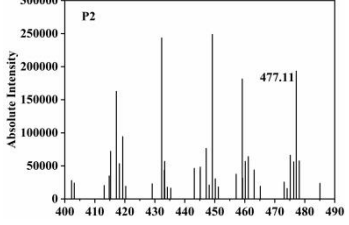
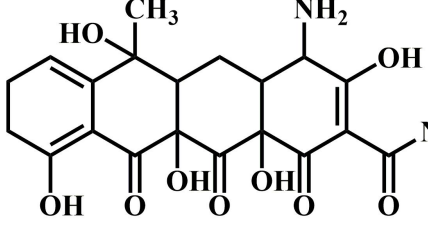
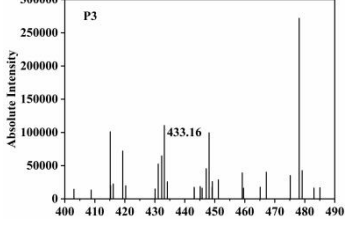
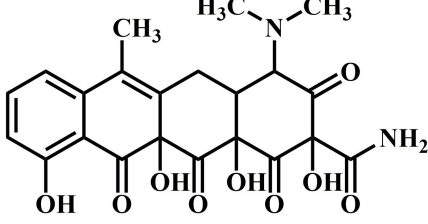
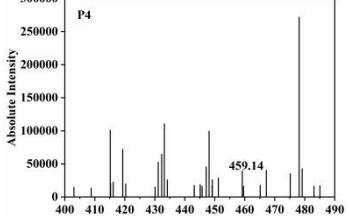
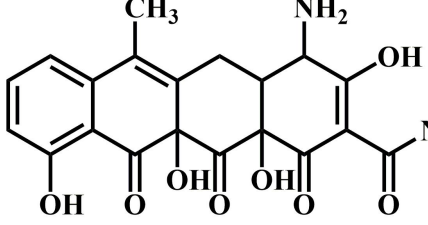
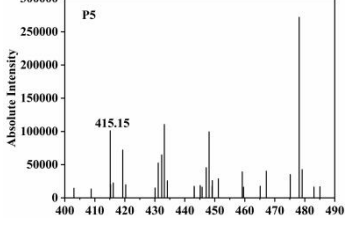


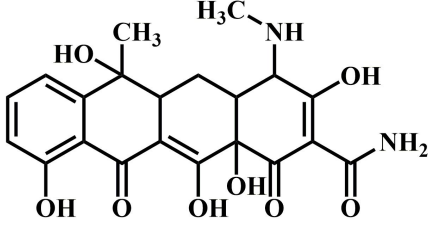
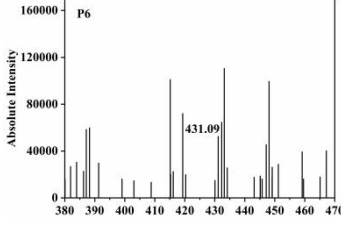
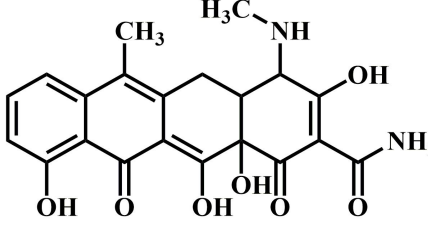
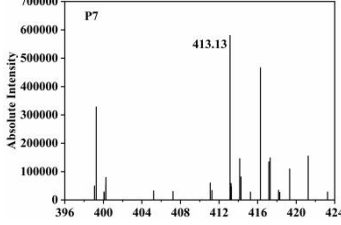
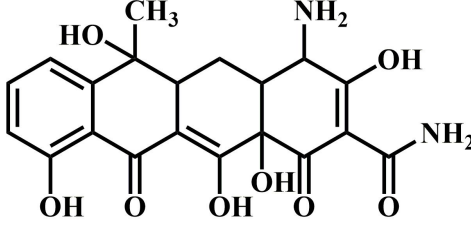
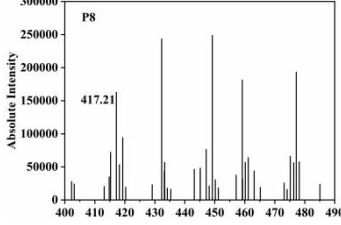
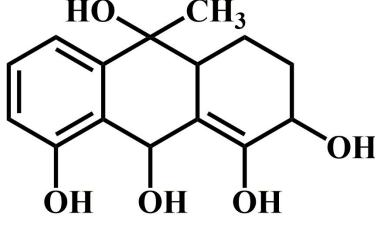
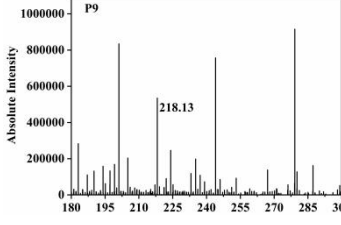
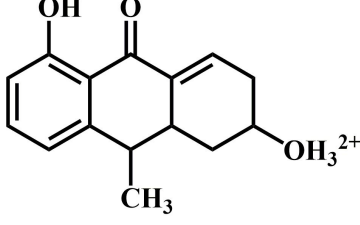
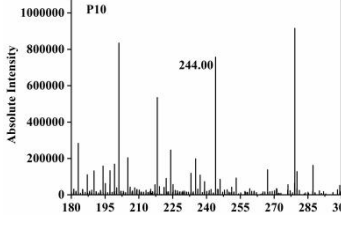
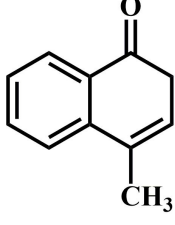
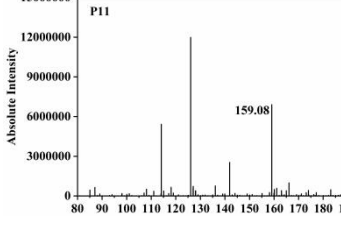
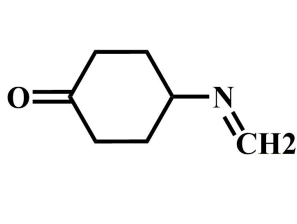
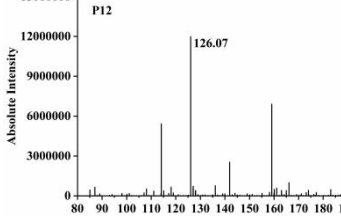
Supplementary Figure 14. EIS spectra for PAF-54 and Ag/AgCl/PAF-54(1:1).

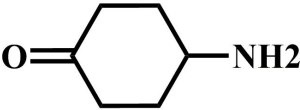
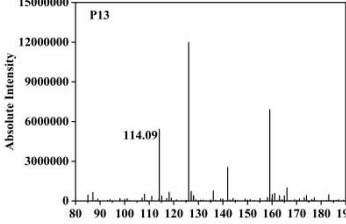


Supplementary Figure 15. (A) Plot of $(ah\nu)^2$ vs. $h\nu$ for band gap of PAF-54; (B) M-S plots of PAF-54.

Supplementary Table 2. LC-MS analysis for intermediates generated in TC degradation in the presence of Ag/AgCl/PAF-54 under visible-light

Name	Mass/Charge (m/z)	Supposed structure(s)	LC-MS data
TC	445.15		
P1	461.11		
P2	478.15		
P3	433.16		
P4	459.14		
P5	415.15		

P6	432.23		
P7	413.13		
P8	416.28		
P9	279.16		
P10	244.00		
P11	159.08		
P12	126.07		

P13	114.09		 <p>Mass spectrum plot for P13. The y-axis is labeled 'Absolute Intensity' and ranges from 0 to 1,500,000. The x-axis ranges from 80 to 190. A significant peak is observed at m/z 114.09, with an intensity of approximately 500,000. Other peaks are visible at m/z 128 (intensity ~1,200,000), 142 (intensity ~300,000), and 156 (intensity ~700,000).</p>
------------	---------------	---	---